

Homogeneity Characterization of Lattice Spacing of Silicon Single Crystals by a Self-Referenced Lattice Comparator at BL-3C

The lattice spacing of a perfect silicon crystal is critical when determining the Avogadro constant by the X-ray crystal density (XRCD) method [1]. In the XRCD method, the Avogadro constant, N_A , is derived from the mean molar mass, M , the density, ρ , and the lattice spacing of the (220) plane, d_{220} , of a perfect silicon crystal using the following equation:

$$N_A = \frac{M}{\rho \times \sqrt{8} \times d_{220}^3}$$

The International Avogadro Coordination (IAC) project started in 2004 has performed various measurements using a silicon crystal highly enriched with ^{28}Si isotope with the aim of achieving an uncertainty of 2×10^{-8} for N_A .

A very important precondition for achieving this goal is to have a perfect silicon crystal or at least an imper-

fect silicon crystal with a known lattice spacing distribution. This is because M , ρ , and d_{220} are measured from samples obtained from different locations in the ingot. Impurity and defect measurements of the crystal are performed for crystal characterization.

The lattice spacing of silicon is determined by combining the lattice spacing measured using a technique that involves X-ray and optical interferometry under standard conditions (i.e., 20°C and 0 Pa). The lattice spacing is required to have an expanded uncertainty of 3×10^{-9} . Impurities measured on samples throughout an ingot are used to derive the compensations at the positions of the X-ray interferometer (XINT) and spheres.

We discovered a strain pattern whose magnitude was of the order of 10^{-8} , which is too small to be observed by X-ray topography, in an ingot of a high-purity silicon crystal with natural isotopic abundances [2].

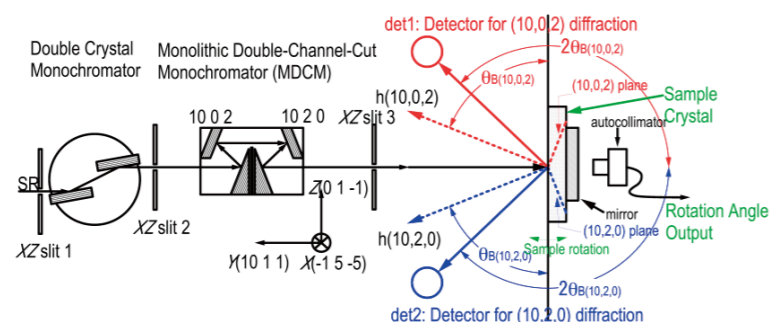


Figure 1
Schematic side view of the self-referenced lattice comparator.

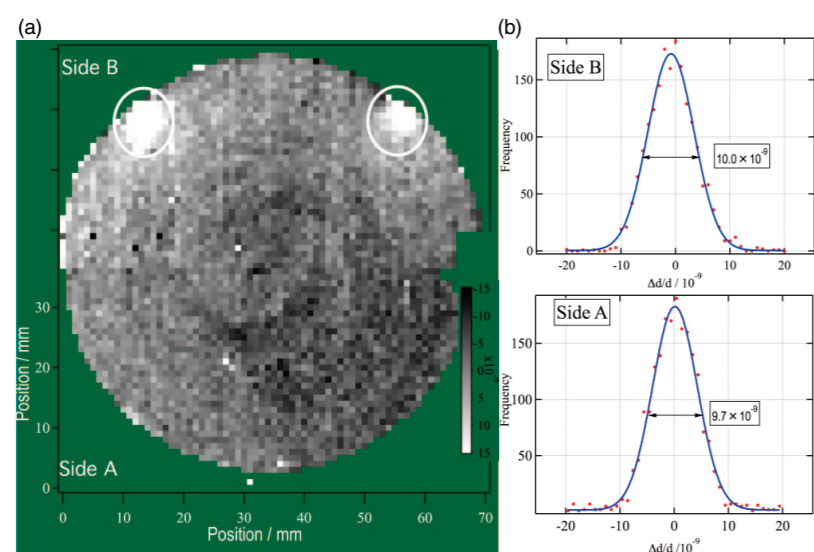


Figure 2
Lattice spacing of ^{28}Si isotopically enriched silicon on both sides of the disk. (b) Histograms of the mapping measurement results.

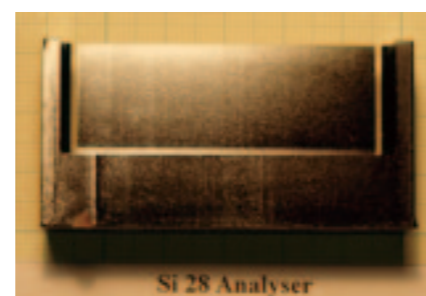


Figure 3
Photograph of the analyzer crystal of XINT (upper side is side B).

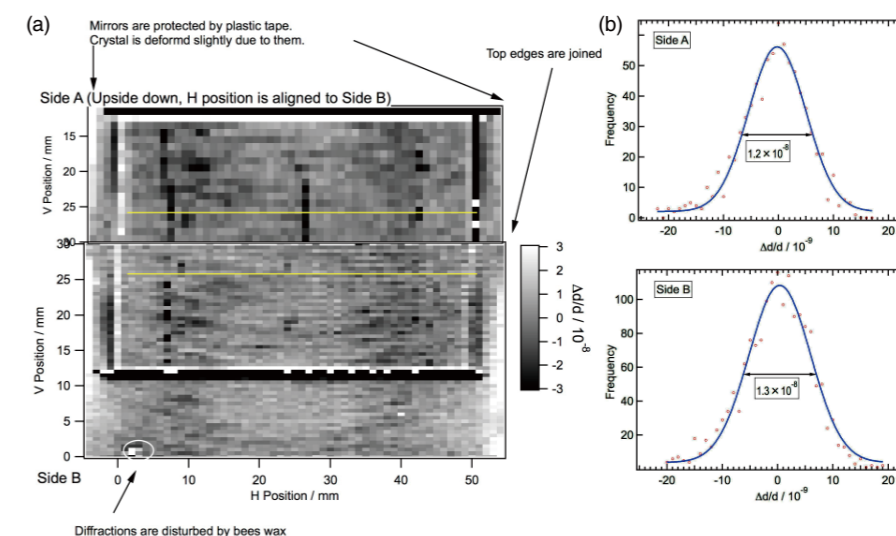


Figure 4
(a) Lattice spacing of the analyzer crystal of XINT from ^{28}Si isotopically enriched silicon. Yellow lines indicate data in Figure 5. (b) Histogram of the mapped data. Only data from the thin plate are used in calculations.

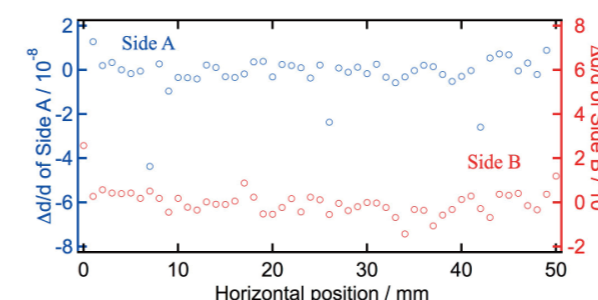


Figure 5
1D maps of the lattice spacing along the baseline. Data were obtained from the mapping data for the yellow lines in Figure 4(a). Horizontal position increases from left to right when the sample is viewed from side B.

This strain distribution has a high spatial frequency in the ingot and thus cannot be compensated by solely determining impurity concentrations at a few sampled positions. Crystals used in X-ray interferometry are also susceptible to the very small strains caused by defects introduced during crystal processing. Damage caused during fabrication and self-weight (gravity-induced) deformation of the crystal must be checked by a sensitive method. Strain measurements were performed [3] using the Self-Referenced Lattice Comparator (SRLC) installed at BL-3C, on single crystals of silicon with natural isotopic abundances, and silicon crystals highly enriched with the ^{28}Si isotope, which are all used to determine the Avogadro constant. A schematic side view of the apparatus is shown in Fig. 1.

The measurement capability, i.e. the standard deviation of repeated measurements, of the system is about 3×10^{-9} [4]. Samples from crystals with natural isotopic abundances exhibited clear pattern of striations, whereas almost no pattern was observed for crystals enriched with ^{28}Si isotope (see Figs. 2, 3, 4 and 5).

The standard deviation of the lattice spacing of the silicon single crystal highly enriched with ^{28}Si isotope was 4.7×10^{-9} , which enabled the lattice spacing to be determined with an expanded uncertainty of 3×10^{-9} .

The Avogadro constant N_A is determined from the measurements, the lattice parameter, the mass and volume of the sphere, and the molar mass to be $N_A = 6.022 140 78(18) \times 10^{23} \text{ mol}^{-1}$ with 3.0×10^{-8} relative uncertainty. This value differs by $16 \times 10^{-8} N_A$ from the CODATA 2006 adjusted value. This value is midway between the N_A values derived from Planck's constant obtained by NIST and NPL watt-balance using the molar Planck constant $N_A h = 3.990 312 682 1(57) \times 10^{-10} \text{ J s/mol}$ [5].

REFERENCES

- [1] B. Andreas, Y. Azuma, G. Bartl, P. Becker, H. Bettin, M. Borys, I. Busch, P. Fuchs, K. Fujii, H. Fujimoto, E. Kessler, M. Krumrey, U. Kuetgens, N. Kuramoto, G. Mana, E. Massa, S. Mizushima, A. Nicolaus, A. Picard, A. Pramann, O. Rienitz, D. Schiel, S. Valkiers, A. Waseda and S. Zakel, *Metrologia*, **48** (2011) S1.
- [2] H. Fujimoto, A. Waseda, Z. Xiaowei, K. Nakayama, K. Fujii, H. Sugiyama and M. Ando, Precision Electromagnetic Measurements, 2002. Conference Digest 2002 Conference on 304 (2002); Digital Object Identifier:10.1109/CPEM.2002.1034842.
- [3] H. Fujimoto, A. Waseda and X.W. Zhang, *Metrologia*, **48** (2011) S55.
- [4] X. Zhang, H. Sugiyama, M. Ando, Y. Imai and Y. Yoda, *J. Appl. Cryst.*, **36** (2003) 188.
- [5] B. Andreas, Y. Azuma, G. Bartl, P. Becker, H. Bettin, M. Borys, I. Busch, M. Gray, P. Fuchs, K. Fujii, H. Fujimoto, E. Kessler, M. Krumrey, U. Kuetgens, N. Kuramoto, G. Mana, P. Manson, E. Massa, S. Mizushima, A. Nicolaus, A. Picard, A. Pramann, O. Rienitz, D. Schiel, S. Valkiers and A. Waseda, *Phys. Rev. Lett.*, **106** (2011) 030801.

BEAMLINER 3C

H. Fujimoto¹, A. Waseda¹ and X.W. Zhang² (¹AIST, ²KEK-PF)